Experimental validation of a computational screening approach to predicting redox potentials for a diverse variety of redox-active organic molecules

Alexandra R. McNeill[1], Samantha E. Bodman[2], Amy M. Burney[1], Chris D. Hughes[1], Deborah L. Crittenden[1,*]

1. School of Physical and Chemical Sciences, University of Canterbury, Christchurch, New Zealand

2. Department of Chemistry, Loughborough University, Loughborough, United Kingdom

* Corresponding author e-mail: deborah.crittenden@canterbury.ac.nz

Abstract

Organic redox flow batteries are currently the focus of intense scientific interest, because they have the potential to be developed into low cost, environmentally sustainable solutions to the energy storage problem that stands in the way of widespread uptake of renewable power generation technologies. Because the search space of suitable redox-active electrolytes is large, computational screening is increasingly being employed as a tool to identify promising candidates. It is well known in the computational chemistry literature that redox potentials for organic molecules can be accurately calculated on a class-by-class basis, but the general utility and accuracy of the relatively low-cost quantum chemical methods used in high-throughput screening is currently unclear. In this work, we measure the redox potentials of 24 commonly available but chemically diverse redox-active organic molecules in acetonitrile, carefully controlling experimental errors by using an internal reference (the ferrocene/ferrocenium redox couple), and compare these with redox potentials computed at B3LYP/6-31+G(d,p) using a polarizable continuum model to account for solvation. Unlike previous large-scale computational screening studies, this work carefully establishes the accuracy of the computational procedure by benchmarking against experimental results. While previous small-scale computational studies have been carried out on structurally homologous compounds, this work assesses the accuracy of the computational model across a variety of compound classes, without applying class-dependent empirical corrections. We find that redox potential differences for coupled one-electron transfer processes can be computed to within 0.4 V and two-electron redox potential differences can usually be computed to within 0.15 V.

Introduction

In the quest to reduce the amount of atmospheric carbon dioxide and other greenhouse gases exacerbating climate change, the world is experiencing an increase in power generation from low-carbon, renewable sources such as solar and wind. While these methods of electricity generation do not involve the burning of fossil fuels, their fluctuating electrical output, affected by time of day and weather conditions, does not match up with the demand from consumers. As such, methods of storing the generated electricity are required to be able to feed the power into the grid when needed. One type of large-scale secondary battery that could be capable of doing this is the redox flow battery (RFB). RFBs consist of a redox-active pair contained in separate external tanks and flowed past each other in a central electrochemical cell, separated by an ion-exchange membrane. Although they have lower energy densities than other batteries such as Li-ion,[1] they are desirable due to their safety, longevity, and flexibility of design. It is this latter parameter which many research groups have been studying; chemical components such as solvent,[2,3] redox-active species,[4] and supporting electrolyte[5] are of importance, as are the engineering aspects including membrane,[6–8] cell design,[9] and electrodes.

The first RFBs were based on vanadium redox pairs in aqueous solution.[10] While water is a safe, cheap and non-flammable solvent choice for RFBs, the conditions required for good performance are often either extremely acidic or basic.[1] Furthermore, the relatively narrow electrochemical stability window of water limits the available voltage of the battery as the redox pair must be active within this window. A solvent with a larger electrochemical stability window would allow a broader range of electroactive species to be considered and, depending on the separation of their reduction/oxidation potentials, may result in an RFB with a larger voltage than possible with an aqueous RFB. However, the solubility of salts in non-aqueous solvents is often poor,[2] resulting in lower Coulombic capacity. To ensure that non-aqueous RFBs can achieve useful power capacities, it is important to optimize voltage using the full electrochemical stability window of the solvent. This means choosing redox-active pairs that have the largest possible redox potential difference. There are already many redox-active organic compounds available cheaply on an industrial scale; they are commonly used in applications such as pH indicators,[11] pharmaceuticals,[12] herbicides,[13] and dyes.[14] It is worthwhile to examine species in these areas and extend the search for organic RFB active species beyond those which have already been well-studied and derivatised, like viologens and anthraquinones.[15–21] As RFB research in the area of organic redox-active species progresses, one of the tools that can streamline this process is computational chemistry.

Using computational methods to predict the reduction and/or oxidation potentials of redox-active molecules is not a new approach. Early models correlated observed redox potentials against Hammett parameters.[22,23] More recently, empirical relationships between experimental redox potentials and

HOMO-LUMO gap energies have been established.[24,25] However, for fully *ab initio* predictions of redox potentials, it is necessary to compute the free energy difference between the oxidised and reduced forms of the molecule, as well as the corresponding quantities for a specified reference system - typically the standard hydrogen electrode.[26–29]

Using this approach, large-scale computational screening studies have been carried out to identify promising RFB species, [27–29] but these lack experimental validation. Joint computational and theoretical studies, on the other hand, typically only focus on a single class of molecules.[30–36] By way of example, correlations between predicted and measured redox potentials from the literature are illustrated in Figure 1. Although each individual study shows good agreement between theory and experiment, these studies use quite different computational and experimental approaches (Table 1), which makes it hard to draw generalised conclusions about the ability of any given computational method to predict experimental redox potentials for a wide range of compounds.

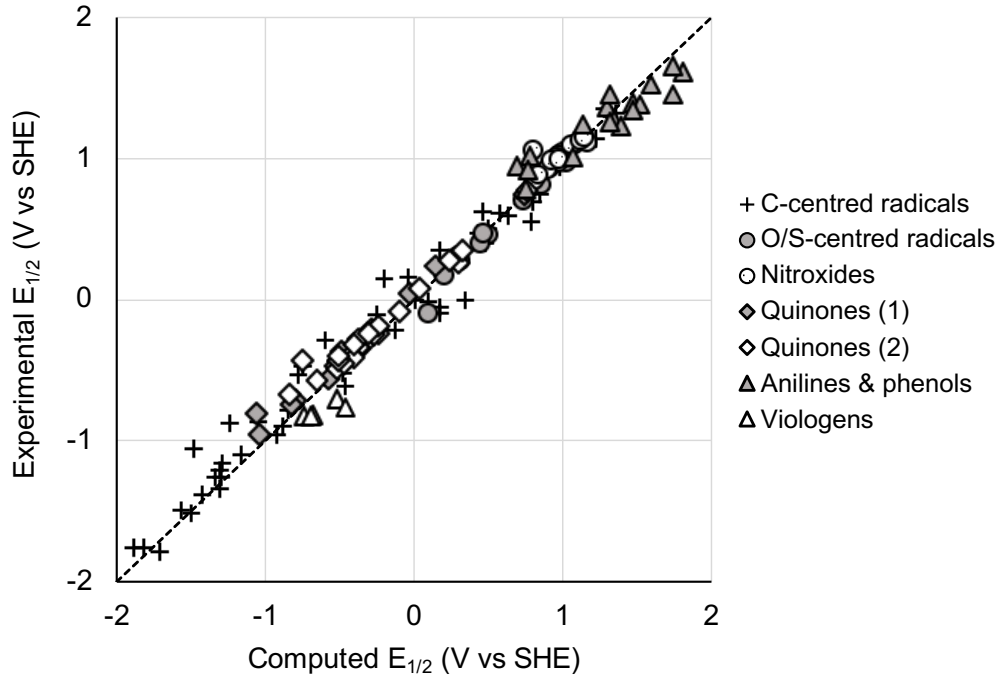

Figure 1. Computed vs experimental oxidation and reduction potentials for 136 redox-active organic molecules, compiled from the literature.[30–36]

Experimentally, results can vary according to choice of reference electrode, supporting salt, concentrations of electrolytes, solvent, and voltammetric technique. Further, corrections are required to express both computed and measured redox potentials relative to the standard hydrogen electrode, and there is some uncertainty associated with how these values are derived or measured.

Uncertainties in measured redox potentials can be as large as 1 V,[35] but for carefully controlled experimental studies, uncertainties of < 0.1 V are more common.[26,33–35]

Table 1. Key parameters and correction factors that influence the accuracy of reported experimental and computational redox potentials. Comments in italics refer to post-hoc corrections applied to the published literature values of both computational and experimental redox potentials to ensure consistent referencing against the standard hydrogen electrode.

Species &	**Experimental**		**Computational**		
Process	**Electrode**	**Solvent**	**Method (gas//solv)**	**Solvent**	**Notes**
C-centred radical oxidation[30]	SCE (+0.24 to SHE)	MeCN	B3LYP/ 6-311++G(2df,2pd) (4.44 to SHE)	PCM (ε = 37.5)	Empirical offset of +0.28 V applied to computational E^o
O/S-centred radical reduction[31]	SCE (+0.241 to SHE)	MeCN	G3MP2// B3LYP/6-31+G(d,p) (-4.43 to SHE)	PCM (ε = 37.5)	Solvation model uses modified atomic radii
Nitroxide radical oxidation[32]	Ag/Ag^+ (+0.271 to SCE)	MeCN	G3MP2-RAD// B3LYP/6-31+G(d) (4.52 to SHE)	PCM (ε = 37.5)	
Quinone (1) reduction[33]	SCE	MeCN	G3MP2-RAD// B3LYP/6-31+G(d) (-4.67 to SCE)	CPCM (ε = 37.5)	*+0.24 V added to all literature values to reference to SHE*
Quinone (2) reduction[34]	Fc/Fc^+	MeCN	B3LYP/6-31++G(d,p) (reference reaction potential set to experimental value)	CPCM (ε = 37.5)	*+0.64 V added to all literature values to reference to SHE*
Aniline and phenol oxidation[35]	SHE	H_2O	DLPNO-CCSD(T)/def2-SVP/TZVP(extrap) (4.28 to SHE)	Explicit	Experimental redox potentials carefully curated from literature
Viologen reduction[36]	Ag/AgCl (-0.23 to SHE)	H_2O	B3LYP/6-31+G(d,p) (-4.42 to SHE)	CPCM (ε = 78.2)	

Of the computational studies included amongst these examples, only the Sterling and Bjornsson predictions of aniline and phenol oxidation potentials[35] are truly *ab initio,* i.e. aim to recover experimental redox potentials directly, without relying on parameters built in to implicit solvation models and/or using electrode potential referencing schemes that cannot be fully justified *ab initio* and/or applying empirical corrections to improve agreement between computed and observed redox potentials. Yet despite its high computational cost, this approach yields a relatively poor correlation between computed and observed redox potentials; in Figure 1, the "anilines and phenols" data shows substantial deviation from and scatter about the diagonal equivalence line.

In contrast, redox potentials predicted using DFT and/or composite *ab initio* methods with implicit solvation corrections appear to be at least as accurate, but can be obtained at much lower computational cost. However, it is hard to establish their true accuracy, because offsets have been

applied that simultaneously account for electrode referencing and compensate for semi-systematic electronic structure and/or solvation model errors that cancel within an homologous series but not across a wider range of compounds.[26,37] The semi-empirical nature of density functionals and implicit solvation models means that their accuracy depend on the charge state/s of the redox species of interest, whether the redox species of interest is open- or closed-shell,[31] whether the charge of an ion is localised or delocalised, or in general where the computational model at hand does not describe a particular type of species as well as it does another, *e.g.* where implicit solvation model parameters are better suited to one class of compounds than another.[26]

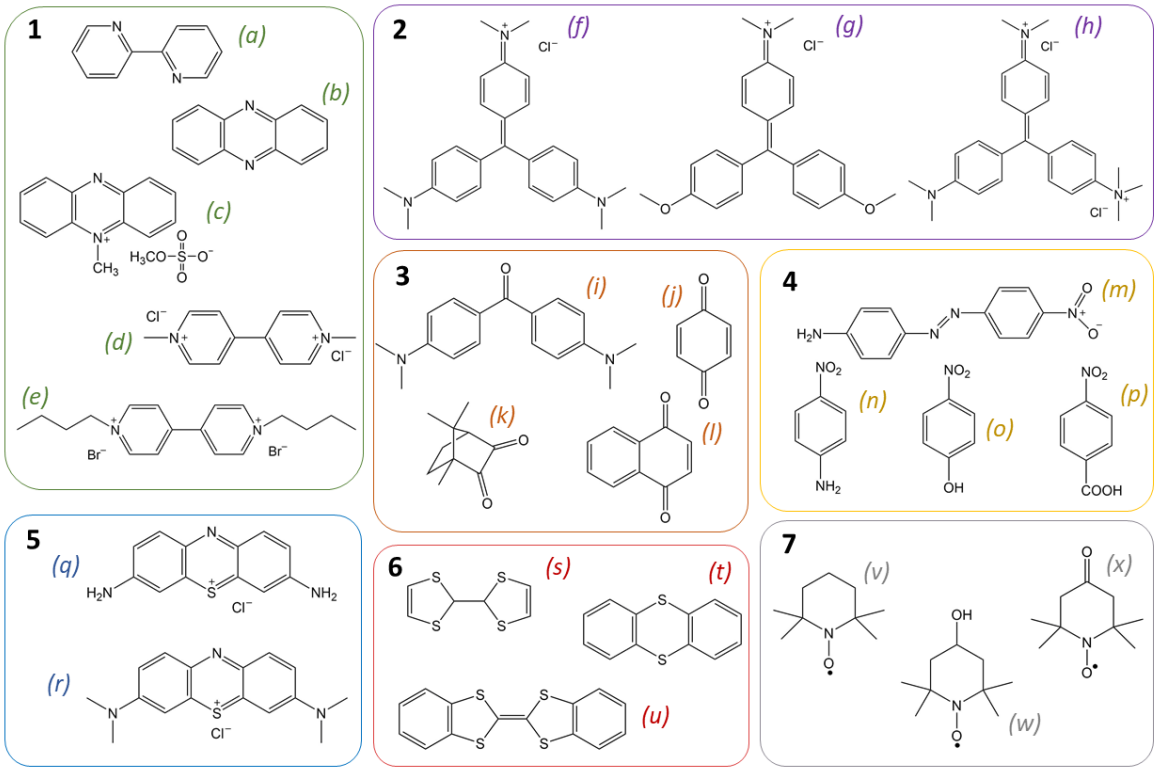

Figure 2. Chemical species investigated in this work, separated into categories. 1. Viologens and similar; 2. Triarylmethanes; 3. Quinones and ketones; 4. Nitroaromatics; 5. Phenothiazines; 6. Chalcogens; 7. TEMPO analogues. Their titles as referred to in this work are listed below the structures.

In this work, we aim to resolve these questions of accuracy, reliability and generalisability through a joint experimental and computational investigation into the redox activity of a diverse set of organic molecules with potential applications in redox flow batteries. Our data set comprises 24 active species across 7 different compound classes, as illustrated in Figure 2. A primary focus of this work is to establish and validate computationally efficient procedures for predicting relative redox potentials

that can be used by chemists without extensive computational chemistry experience using only modest computational resources, *i.e.* a standard desktop PC, employing commonly available and widely used electronic structure and continuum solvation models. We will carefully control experimental and computational referencing in order to quantify and explain residual systematic and random errors in predicted redox potentials, and assess the overall applicability and accuracy of the proposed computational model.

Methods

Computational prediction of redox potentials vs Fc/Fc^+

The geometry of each molecule illustrated in Figure 2, and its oxidised and reduced counterparts, were optimised using the B3LYP method with a 6-31+G(d,p) basis set (QChem 4).[38] Single point solvation stabilization corrections were computed using a conductor-like polarisable continuum model (C-PCM) with a dielectric constant of 37.5 (acetonitrile, MeCN), employing the default atomic radii implemented within QChem. Analogous calculations were performed for ferrocene and ferrocenium, using a radius of 2.928 for Fe within the CPCM model.

Absolute redox potentials were computed as the difference in absolute energies between oxidized reduced forms (in eV), and referenced to the standard hydrogen electrode (SHE) by summing the half-reaction potentials:

Active species reduced, SHE oxidised	**Active species oxidised, SHE reduced**
$A(ox) + e^- \rightarrow A(red)$	$A(red) \rightarrow A(ox) + e^-$
$½\ H_2(g) \rightarrow H^+(solv) + e^-$	$H^+(solv) + e^- \rightarrow ½\ H_2(g)$

Determining the SHE reference potential requires benchmark values for the free energy of formation of atomisation and ionisation of H_2 to form gas phase protons, plus the free energy of solvation of a proton and, optionally, the free energy of reorganisation of solvent upon insertion of charged particles into the solvent medium relative to solvent structuring at the surface (surface potential).[26] This last term is not required if these effects cancel between half-reactions, and we choose to omit it for simplicity and clarity. However, we note that ignoring this term may introduce quasi-systematic errors into the computed redox potentials – dependent on the charge states of the species involved.

Although these quantities are not trivial to compute or measure, substantial research efforts have gone into determining the absolute free energy of reduction of the standard hydrogen electrode in aqueous solution as 4.28 eV (without surface potential correction) or 4.44 eV (with surface potential correction).[26] However, benchmark free energy values are only available for solvation of protons in water. Various estimates for the solvation free energy difference between a proton in water and a

proton in acetonitrile ($\Delta\Delta G_{solv}$) are available,[39] and these lie in the range 0.1 – 0.35 eV for the reaction below as written:

$$H^+(aq) \rightarrow H^+(MeCN)$$

However, given the substantial uncertainty in these estimates, we choose not to apply this correction but instead consider it a source of systematic error when comparing computational predictions and experimental observations of oxidation and reduction potentials.

It remains to align the predicted redox potentials referenced against the standard hydrogen electrode to the measured potentials referenced against the ferrocene/ferrocenium (Fc/Fc^+) redox couple as an internal standard. Once again, estimates of the Fc/Fc^+ redox potential relative to the SHE vary, and can depend on experimental conditions, ranging from -0.624 V to -0.64 V.[40,41] However, because all of our measurements are made under the same experimental conditions, this too will be a potential source of systematic error between theory and experiment, and we simply use the most recent value of -0.64 eV.

We therefore compute redox potentials for active species of interest referenced to Fc/Fc^+ as:

$$E_{½} = |E(ox) – E(red)| – 4.28 – 0.64 \quad (1)$$

Where E(ox) and E(red) are the electronic energies of the oxidised and reduced forms, respectively, in units of electron-Volts (1 E_h = 27.2114 eV).

Alternatively, the absolute redox potential of Fc/Fc^+ may be estimated computationally as:

$$\Delta E_{Fc} = |E(Fc^+) – E(Fc)| \quad (2)$$

This gives a purely computational estimate for the redox potential for the active species of interest referenced to the ferrocene redox couple:

$$E_{½} = |E(ox) – E(red)| – \Delta E_{Fc} \quad (3)$$

At B3LYP/6-31+G(d,p), we find ΔE_{Fc} = 5.13 V, in reasonably close agreement with the value of 4.92 V estimated using the two-step approach above. For consistency with the majority of the existing literature, we will use equation (1) for the remainder of this work. Differences in referencing schemes appear as systematic offsets between computed and experimental redox potentials, so can be easily accounted for.

We note that the energies we obtain computationally do not account for changes in zero point vibrational energy, thermal energy or entropy upon oxidation or reduction, but it has been shown that these effects are very small (< 0.1 eV in aggregate).[37] These are much smaller than the non-systematic errors associated with choice of electronic structure model.[37]

Experimental

Tetrabutylammonium tetrafluoroborate ($TBABF_4$, Alfar Aesar), acetonitrile (MeCN, HPLC grade, Merck), and 4-nitroaniline (Riedel-de Haën) were used as received. Tris(4-(dimethylamino)phenyl) methylium chloride (Crystal Violet), thionine, methylthioninium chloride (Methylene Blue), 4-((4-(dimethylamino)phenyl)(4-(dimethyliminio)cyclohexa-2,5-dien-1-ylidene)methyl)-N,N,N-trimethyl anilinium dichloride (Methyl Green), 4-nitrophenol, and 4-nitrobenzoic acid were sourced from British Drug Houses and used as received. Ferrocene, phenazine, phenazine methosulfate (methylphenazine), methyl viologen, 1,4-naphthoquinone, camphorquinone, 1,4-benzoquinone, 4,4'-bis(dimethylamino)benzophenone (Michler's Ketone), 4-(4-nitrophenylazo)aniline (Disperse Orange 3), tetrathiafulvalene (TTF), dibenzotetrathiafulvalene (dibenzoTTF), thianthrene, 2,2,6,6-tetramethyl-1-piperidinyloxy (TEMPO), 4-oxo-2,2,6,6-tetramethyl-1-piperidinyloxy (oxoTEMPO), and 4-hydroxy-2,2,6,6-tetramethylpiperidin-1-oxyl (hydroxyTEMPO) were sourced from Merck/Sigma Aldrich and used as received. Butyl viologen dibromide and bis(methoxyphenyl)-(dimethylamino)phenyl) methylium chloride (bismethoxy Crystal Violet) were synthesised and characterised by mass spectrometry. Mass spectra were recorded on either a DIONEX ultimate 3000 or Bruker MaXis 4G spectrometer. Characterisation details are reported in the Supporting Information.

Butyl viologen dibromide

To a solution of 4,4'-bipyridine (0.50 g, 3.20 mmol) and acetonitrile (80 mL) was added 1-bromobutane (3.7 mL, 32.00 mmol) and the reaction mixture was heated to reflux overnight. Upon cooling the reaction mixture to room temperature, the yellow solid formed was filtered to give butyl viologen dibromide (46%).

Bis(methoxyphenyl)-(dimethylamino)phenyl)methylium chloride (bismethoxy Crystal Violet)

To a solution of 4-bromo-*N,N*-dimethylaniline (0.48 g, 2.40 mmol) in anhydrous tetrahydrofuran (20 mL) cooled to -78°C, *n*-butyl lithium (1.68 mL, 3.36 mmol, 1.6 M in hexanes) was added dropwise under a nitrogen atmosphere. The mixture was stirred at -78°C for 1 hour, then a solution of 4,4'-dimethoxybenzophenone (0.68 g, 2.80 mmol) dissolved in anhydrous tetrahydrofuran (10 mL) was added. The reaction was allowed to warm to room temperature. The reaction was quenched with water (20 mL), extracted with dichloromethane (3 x 80 mL), and the combined organic fractions were dried (Na_2SO_4,) and concentrated under reduced pressure. The resulting yellow residue was dissolved in methanol (40 mL), acidified with conc. hydrochloric acid (0.5 mL) to give a dark red solution which was concentrated under reduced pressure to give the product (57%).

Cyclic voltammetry

Cyclic voltammetry was performed in a 2 mL glass cell containing 0.1 M tetrabutylammonium tetrafluoroborate in MeCN and ~5 mM of species of interest. The working electrode was a glassy carbon rod with sides encased in Teflon, polished on a suede cloth with a silica slurry. The quasi-reference electrode was a silver wire, and the counter electrode was a Pt coupon. Samples were purged with N_2 for 15 minutes prior to measurement. All cyclic voltammetry was performed at 100 mV/s, using an Autolab potentiostat controlled by Nova 11.1 (Metrohm Autolab). The half-wave potential, $E_{1/2}$, was recorded as the average of the peak potentials of the peak currents of the cathodic and anodic processes. This can be used as an approximation of the formal reduction (or oxidation) potential of that species, which can be compared to the computational prediction. The exception to this was 2,2'-bipyridine, for which the reduction was not reversible; in this case the reduction potential was recorded as the potential of the peak reduction current.

Results and Discussion

The species which were investigated in this study are shown in Figure 2. There are 5 families of species that undergo electrochemical reduction: viologens and other nitrogen-containing systems (1), triarylmethanes (2), quinones and ketones (3), nitro-containing species (4), and phenothiazines (5). The remaining two families are known to undergo reversible electrochemical oxidation: chalcogens (6) and TEMPO derivatives (7). Table 2 outlines the redox reactions characterised in this work.

Table 2. Summary of chemical families which undergo different electrochemical events.

One electron reduction	**Two electron reduction**	**One electron oxidation**	**Two electron oxidation**
Viologens	Viologens	Chalcogens	Chalcogens
Triarylmethanes	Quinones	TEMPOs	
Quinones			
Nitroaromatics			
Phenothiazines			

1-Electron Processes

Computational and experimental $E_{1/2}$ values for all one-electron reduction and oxidation processes are reported in Table 3. The cyclic voltammograms from which the experimental values were derived are provided as Supporting Information. By using an internal reference Fc/Fc^+, some of the difficulties associated with using a standard reference electrode are minimised – such as changes in electrode surface chemistry leading to poor reproducibility, or the formation of liquid junction potentials shifting

the reduction potential of the active species.[42] However, some small shifts in experimental potential may be unavoidable.

Table 3. One- and two-electron $E_{1/2}$ values (V vs Fc/Fc^+) obtained computationally and experimentally, using 5 mM concentration of active species in 0.1 M $TBABF_4$/MeCN. Values in brackets are those calculated accounting for self-protonation. To reference against the standard hydrogen electrode, add 0.64 V to all one-electron redox potentials and 1.28 V to all two-electron redox potentials.

Species	1-electron $E_{1/2}$ (V vs Fc/Fc^+)		2-electron $E_{1/2}$ (V vs Fc/Fc^+)	
	Experimental	Computational	Experimental	Computational
2,2'-Bipyridine	-2.55	-2.75	-	-
Phenazine	-1.58	-1.77	-2.08	-2.78
Methylphenazine	-0.49	-0.69	-1.34	-1.81
Methyl viologen	-0.84	-0.89	-1.24	-1.76
Butyl viologen	-0.90	-1.25	-1.25	-1.46
Crystal Violet	-1.25	-1.61	-	-
Bismethoxy CV	-0.90	-1.28	-	-
Methyl Green	-0.90	-1.22	-	-
Michler's Ketone	-2.51	-2.87	-	-
Camphorquinone	-1.80	-1.72	-	-
Naphthoquinone	-1.00	-1.01	-	-
Benzoquinone	-0.84	-0.74	-1.37	-2.03
Nitrophenol	-2.04	-1.61 (-1.99)	-	-
Nitroaniline	-1.72	-1.76	-	-
Nitrobenzoic acid	-1.54	-1.17 (-1.48)	-	-
Disperse Orange 3	-1.30	-1.28	-1.60	-2.18
Thionine	-0.63	-1.02	-	-
Methylene Blue	-0.70	-1.08	-1.40	-1.95
Tetrathiafulvalene	0.00	-0.37	0.73	0.59
DibenzoTTF	0.19	-0.18	1.27	0.68
Thianthrene	0.86	0.52	-	-
TEMPO	0.25	0.18	-	-
HydroxyTEMPO	0.31	0.23	-	-
OxoTEMPO	0.45	0.45	-	-

Similarly, the supporting electrolyte can influence the reduction or oxidation potential of a species, depending on the ions' ability to stabilise the reduction or oxidised form.[43] Here, the same supporting electrolyte has been used for all experimental studies but will have had slightly different stabilising effects for each species. This should be considered an unavoidable source of semi-random error, although the magnitude of this effect is relatively small (< 0.1 V) in the concentration range used

here.[44] Although the ionic active species have counterions which could also participate in this stabilisation, the low concentration (~5 mM) is unlikely to have a significant effect compared to the 0.1 M concentration of $TBABF_4$.

The correlation between computational and experimental $E_{1/2}$ values is illustrated in Figure 3. There is generally good agreement between computational predictions and experimental measurements (slope = 0.9985 ± 0.0885 [95%CI], R^2 = 0.9613) but closer inspection reveals that the data tend to cluster into two separate categories. For quinones, nitroaromatics and nitroxides there is very close agreement between theory and experiment, with most data points falling on or near the equivalence line. For triarylmethanes, phenothiazines and chalcogens, computational redox potentials are more negative than their experimental counterparts. Only molecules from the viologen/phenazine/pyridine family tend to scatter about the line of best fit. This is perhaps due to the structural and chemical diversity of molecules within this class.

Differences between predicted and observed $E_{1/2}$ values are more clearly illustrated in Figure 4. This analysis reveals two different types of outliers; nitrophenol and nitrobenzoic acid, whose predicted reduction potentials are too positive relative to those of other species in this class, and Michler's ketone and butyl viologen whose predicted reduction potentials are more negative than would otherwise be expected based on their electronic and structural similarity to other species in their respective classes.

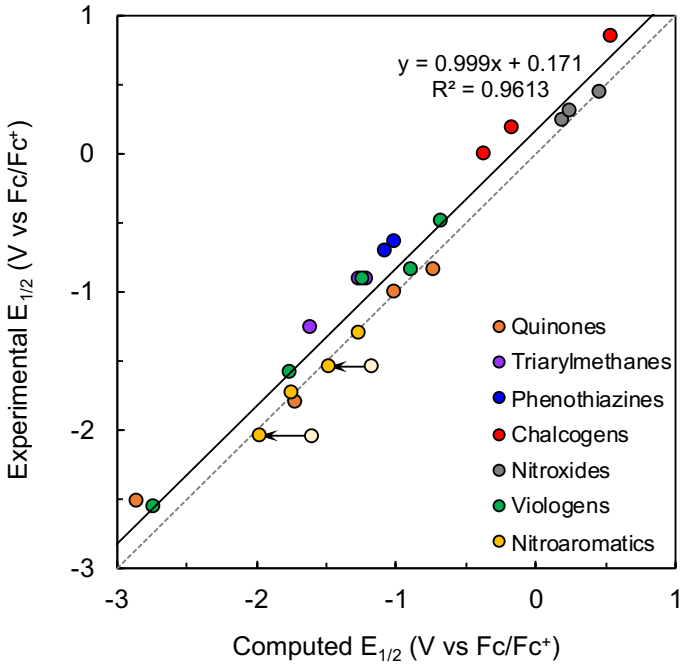

Figure 3. Linear regression analysis of computed and experimental 1-electron $E_{1/2}$ values for a selected group of molecules and ions. Experimental data was obtained using cyclic voltammetry at 100 mV/s in 0.1 M $TBABF_4$, MeCN. Computational values were calculated at B3LYP/6-31+G(d,p) using a continuum solvation model with

dielectric constant of 37.5 (MeCN). For nitrophenol and nitrobenzoic acid, reduction potentials were computed both with (dark yellow, included in regression analysis) and without (light yellow, omitted from regression analysis) accounting for intramolecular proton transfer. The solid black line represents the line of best fit, while the line of equivalence is dashed grey.

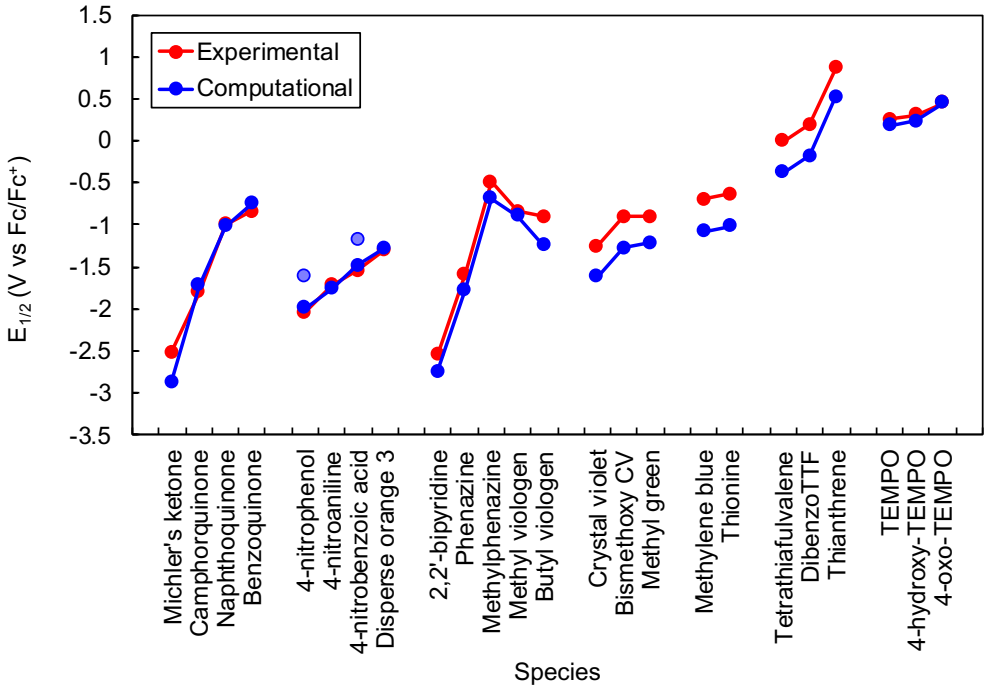

Figure 4. Direct comparison of computational and experimental $E_{1/2}$ values as referenced to the Fc/Fc^+ couple. Experimental data was obtained using cyclic voltammetry at 100 mV/s in 0.1 M $TBABF_4$, MeCN. Blue shaded points represent predicted redox potentials for 4-nitrophenol and 4-nitrobenzoic acid prior to intermolecular proton transfer. Lines are to guide the eye.

It is known that nitrophenol and nitrobenzoic acid can undergo self-protonation, in which the proton migrates from the acidic functional group (hydroxyl or carboxylic acid) to protonate the nitro substituent.[45] Without considering self-protonation, the computed reduction potential of nitrophenol in MeCN is -1.61 V vs Fc/Fc^+, more positive than the -2.04 V observed experimentally. This result is particularly incongruent, because our computational model tends to predict redox potentials more negative than those obtained experimentally. However, once self-protonation is accounted for in the computational model, the predicted value of -1.99 V agrees almost exactly with experiment. Similarly, the predicted redox potential for nitrobenzoic acid is only consistent with experiment once self-protonation is accounted for.

Michler's ketone and butyl viologen are among the largest molecules investigated here, and by far the most flexible. Therefore, the chances of non-systematic methodological errors being introduced during the geometry optimization process are greatest for these species. In particular, linear dependence in the atomic orbital basis set is often a problem for large molecules when the basis set is augmented with diffuse functions, and this extent of linear dependence can vary substantially with molecular geometry. This is not a problem if the geometries of the oxidised and reduced forms are

very similar but can be a problem if the molecules undergo substantial conformational change upon oxidation/reduction.

Two solutions are possible: 1. Using truncated model systems (e.g. the computed redox potentials for methyl viologen are a better predictor of the experimental butyl viologen values than those computed for butyl viologen itself), and 2. Only using diffuse functions when absolutely required, i.e. when modelling anionic species. However, in the interests of ensuring our computational model is easy to define and apply, we instead choose to simply note that these errors may occur and thus introduce uncertainties of around 0.4 V in computed redox potentials.

For the other quinones, predicted redox potentials agree very closely with experimental values. The same is true for other compounds with relatively localised radical states – nitroxides, nitroaromatics and – to a lesser extent – viologens. However, this close agreement is almost certainly due to fortuitous error cancellation. We have not attempted to correct for the differential solvation free energy of a proton in water and acetonitrile in computing the absolute reduction potential of the standard hydrogen electrode, nor systematic errors associated with our choice of electronic structure model and basis set, nor experimental uncertainties associated with referencing to the Fc/Fc^+ redox couple.

For redox species with delocalised radical states – triarylmethanes, phenothiazines and chalcogens – these errors no longer cancel and predicted redox potentials are uniformly ~ 0.4 V more negative than corresponding experimental values. This relationship appears to be independent of the charge state of the parent molecule, whether it is a radical or closed-shell species and/or whether it undergoes oxidation or reduction.

This clear distinction and consistent behaviour makes it tempting to apply separate correction factors for each super-set of molecules. However, there are two problems with this. Firstly, it is not necessarily always clear *a priori* which class a given compound would fall into, and indeed it seems that the viologens fall between them. Secondly, and more importantly, we are interested in establishing a general computational procedure that can be applied without any system-specific knowledge. Overall, we consider it more useful to be able to quantify prediction uncertainties than remove them.

The simplest approach is to simply accept that any given computational prediction may be in error by up to 0.4 V, and relative redox potentials for inter-species redox reactions may also incur errors of up to 0.4 V. It may be possible to reduce errors in computed $E_{1/2}$ values by adding a systematic offset derived from linear regression analysis, but it's important to ensure that this is physically justified and truly accounts for systematic model deficiencies, e.g. neglecting the differential solvation energy of

the proton in acetonitrile vs water. Fortunately, we have an additional source of data to analyse the error profile; computed and observed redox potentials for two-electron processes.

2-Electron Processes

Some redox-active species can undergo multiple reversible redox processes. In some cases, where the second (or third) electron transfer being more thermodynamically favourable than the first, the difference in potential of these steps is so small that they appear as one redox couple on the resulting cyclic voltammogram.[46] In cases where the second electron transfer is less favourable than the first, the peak separation between the two steps increases, allowing two (or more) peaks to appear in the cyclic voltammogram.

In this work, reversible two-electron reductions were seen for the phenazines, viologens, naphthoquinone, benzoquinone, Methylene Blue, and Disperse Orange 3, and two-electron oxidations were seen for TTF and dibenzoTTF. Thianthrene can, under very dry conditions, undergo a second reversible oxidation, but this was not observed here.[47]

Measured potentials for the second redox processes are compared to computational predictions in Figures 5 and 6. Although the correlation between computed and observed redox potentials is slightly stronger than in the one-electron case (R^2 = 0.9788 vs 0.9613), the line of best fit is no longer parallel to the line of equivalence (slope = 0.916 vs 0.999).

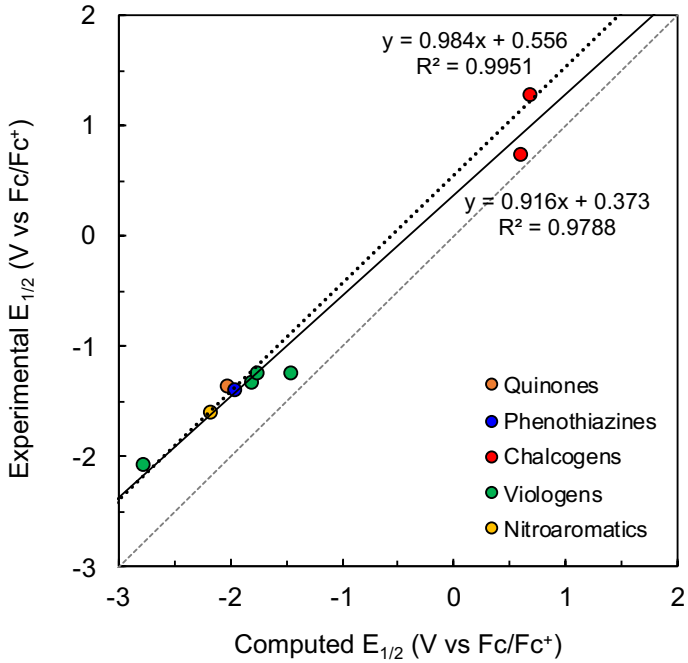

Figure 5. Linear regression analysis of computed and experimental 1-electron $E_{1/2}$ values for a selected group of molecules and ions. Experimental data was obtained using cyclic voltammetry at 100 mV/s in 0.1 M $TBABF_4$, MeCN. Computational values were calculated at B3LYP/6-31+G(d,p) using a continuum solvation model with dielectric constant of 37.5 (MeCN). The solid black line represents the line of best fit to the whole data set, while

the dotted line is fitted to all data points except the outliers butyl viologen (green) and tetrathiafulvalene (red). The line of equivalence is dashed grey.

However, due to the smaller size of the data set, uncertainties in the slope and intercept are also larger. Linear regression parameters for one- and two-electron processes are summarised in Table 4.

Table 4. Linear regression parameters describing correlations between computed and experimental redox potentials for one- and two-electron transfer processes. Reported uncertainties represent 95% confidence intervals.

	1-electron	2-electron	2e, no outliers
slope	0.999 ± 0.089	0.916 ± 0.121	0.984 ± 0.080
intercept	0.17 ± 0.12	0.37 ± 0.22	0.56 ± 0.16
R^2	0.9613	0.9788	0.9951

This behaviour can be traced back to anomalous predictions of redox potentials for the second electron transfer process in butyl viologen and tetrathiafulvalene, as illustrated in Figure 6.

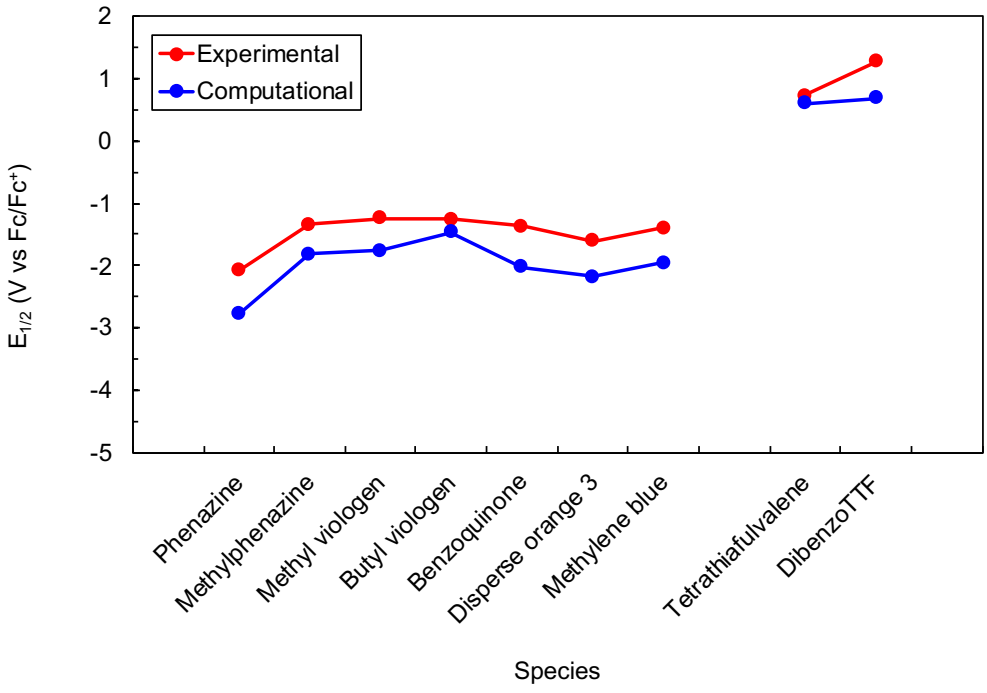

Figure 6. Comparison of computed and experimental $E_{1/2}$ values for a selected group of molecules and ions. Experimental data was obtained using cyclic voltammetry at 100 mV/s in 0.1 M $TBABF_4$, MeCN and referenced to an internal Fc/Fc^+ couple. Computational values were calculated at B3LYP/6-31+G(d,p) using a continuum solvation model with dielectric constant of 37.5 (MeCN).

As in the one-electron case, the anomalous prediction for butyl viologen is likely due to its size and structural flexibility. Linear dependencies due to the presence of diffuse functions in the 6-31+G(d,p)

basis set can give rise to errors that do not cancel between the oxidised and reduced forms. It is well known in the computational chemistry literature that diffuse functions are required for describing the energies and properties of anions,[48–50] but can cause problems when used in computing the electronic energies of cations and uncharged species.[51–53] During the reduction of viologens, all species involved are either cationic or uncharged.

This may also explain the anomalous computed oxidation potential for tetrathiafulvalene, which also undergoes conformational change upon oxidation to its dicationic state, in which the central double bond is formally broken, allowing distortion from planarity.[54] Again, all species involved in the two-electron oxidation of TTF are either cationic or uncharged.

Repeating the linear regression analysis with these two outliers removed shows a much stronger correlation between computed and observed redox potentials (R^2 = 0.9951) with a near-constant offset of ~ 0.56 V. For one-electron redox potentials, on the other hand, an offset of + 0.17 V could be applied to minimize differences between computed and observed redox potentials, although this results in a strongly bimodal distribution of residuals. Clearly, it is not possible to apply a single correction offset that accounts for systematic errors in *both* one- and two-electron redox potential predictions.

RFB design implications

Therefore, in the interests of clarity and consistency, we choose not to apply any post-hoc corrections to the predicted redox potentials obtained here. We recommend that further computational studies are carried out to accurately determine the solvation energy of a proton in acetonitrile, analogous to those already available in the literature that provide benchmark values for aqueous proton solvation free energies.[55,56] We anticipate that this will provide a solid foundation for applying systematic corrections that will better align theory and experiment in a non-empirical manner, and enable remaining computational method errors to be isolated and quantified.

Fortunately, in the context of designing redox flow batteries, we do not need accurate absolute redox potentials because we are primarily interested predicting redox potential differences to predict open-cell voltages when different redox pairs are combined.

Overall, finding complementary species that undergo two-electron oxidation and reduction reactions is desirable from both a theoretical and practical point of view. Theoretically, redox potential differences for these species can be determined quite accurately in most cases where systematic deviations from experiment cancel. Practically, two-electron redox processes are desirable because this maximises redox potential differences and increases the total amount of energy that can be stored.

However, electrochemical reversibility cannot be predicted computationally. This is particularly pertinent for the second electron transfer process which is more likely to be irreversible than the first. There is also not necessarily any particular relationship between chemical structure and electrochemical reversibility. For example, both of the phenazine compounds participated in two reduction events, but only for methyl phenazine was this reversible. Similarly, even the single-electron reduction of 2,2'-bipyridine was irreversible despite its structural similarly to the phenothiazines and viologens.

In aprotic conditions, nitrobenzene is known to undergo a two one-electron reductions: the first reduction forms the radical anion, and the second, the dianion.[46] This same process appears to occur during the cyclic voltammetry of Disperse Orange 3 (cyclic voltammogram provided in Supporting Information). The reversibility of the second step is highly dependent on the environment, as the dianion reacts readily with solvent and impurities. While the second electron reduction appears reversible in this case, it is likely that after continued cycling of Disperse Orange 3 at low potentials, the second reduction would become irreversible.

Experimental conditions also affect the electrochemical reversibility of thianthrene oxidation. Under very dry conditions, thianthrene is known to undergo reversible one- and two-electron oxidation.[47] While our experimental value of +0.86 V vs Fc/Fc^+ for one-electron oxidation is in line with literature results, we do not observe the second oxidation process seen in previous work.[47]

Finally, it is important to carefully consider whether the redox species of interest can undergo side-reactions upon oxidation/reduction, from both an experimental and computational modelling perspective. For example, nitrophenol undergoes an irreversible reduction process at -1.5 V vs Fc/Fc^+, followed by a reversible reduction at -2.04 V vs Fc/Fc^+. We now understand that this first process corresponds to reduction plus intramolecular proton transfer and the second process is reduction of the protonated-nitro form. Nitrobenzoic acid exhibits the same behaviour.

This illustrates a potential pitfall of blindly applying computational redox potential screening procedures, even if other sources of error can be eliminated (by computing redox potential differences so that they cancel) or otherwise accounted for (by applying physically-motivated and externally-validated correction offsets).

Conclusion

Although we have not attempted to perform a large-scale computational screening study in this work, we have nonetheless surveyed a substantial variety of redox-active organic molecules, and carefully measured their redox potentials under consistent experimental conditions using the Fc/Fc^+ redox

couple as an internal reference to eliminate sources of experimental variability. We have also validated a straightforward and relatively low-cost computational procedure for predicting relative redox potentials for coupled one-electron transfer processes to within 0.4 V and coupled two-electron transfer processes to within 0.15 V, except those involving outliers where structural flexibility and basis set linear dependency errors can combine to produce errors of up to 0.56 V. This can potentially be avoided by using truncated model systems (e.g. methyl viologen as a model for butyl viologen) and/or considering only structurally rigid molecules. Further work is required to disentangle the different sources of systematic error in one- and two-electron redox potential predictions. Benchmark values for solvation energy of a proton in acetonitrile would be useful to isolate and identify the remaining referencing and computational method errors.

Supporting Information

Chemical structures of redox species and their computationally optimized geometries and electronic energies, cyclic voltammograms, experimental synthesis and characterisation details for butyl viologen and bis-methoxy Crystal Violet, computational and experimental redox potentials compiled from the literature.

Acknowledgements

Financial support for this work was provided through the School of Physical and Chemical Sciences, University of Canterbury and Callaghan Innovation.

References

(1) Winsberg, J.; Hagemann, T.; Janoschka, T.; Hager, M. D.; Schubert, U. S. Redox-Flow Batteries: From Metals to Organic Redox-Active Materials. *Angewandte Chemie - International Edition* **2017**, *56* (3), 686–711. https://doi.org/10.1002/anie.201604925.

(2) Attanayake, N. H.; Kowalski, J. A.; Greco, K.; Casselman, M. D.; Milshtein, J. D.; Chapman, S. J.; Parkin, S. R.; Brushett, F. R.; Odom, S. A. Tailoring Two-Electron Donating Phenothiazines to Enable High Concentration Redox Electrolytes for Use in Nonaqueous Redox Flow Batteries. *Chemistry of Materials* **2019**. https://doi.org/10.1021/acs.chemmater.8b04770.

(3) Navalpotro, P.; Palma, J.; Anderson, M.; Marcilla, R. Exploring the Versatility of Membrane-Free Battery Concept Using Different Combinations of Immiscible Redox Electrolytes. *ACS Applied Materials & Interfaces* **2018**, *10* (48), 41246–41256. https://doi.org/10.1021/acsami.8b11581.

(4) Kosswattaarachchi, A. M.; Cook, T. R. Concentration-Dependent Charge-Discharge Characteristics of Non-Aqueous Redox Flow Battery Electrolyte Combinations. *Electrochimica Acta* **2018**, *261*, 296–306. https://doi.org/10.1016/j.electacta.2017.12.131.

(5) Roznyatovskaya, N.; Noack, J.; Mild, H.; Fühl, M.; Fischer, P.; Pinkwart, K.; Tübke, J.; Skyllas-Kazacos, M. Vanadium Electrolyte for All-Vanadium Redox-Flow Batteries: The Effect of the Counter Ion. *Batteries* **2019**, *5* (1), 1–16. https://doi.org/10.3390/batteries5010013.

(6) Shin, S.; Yun, S.; Moon, S. A Review of Current Developments in Non-Aqueous Redox Flow Batteries: Characterization of Their Membranes for Design Perspective. *RSC Advances* **2013**, *3*, 9095–9116. https://doi.org/10.1039/c3ra00115f.

(7) Su, L.; Darling, R. M.; Gallagher, K. G.; Xie, W.; Thelen, J. L.; Badel, A. F.; Barton, J. L.; Cheng, K. J.; Balsara, N. P.; Moore, J. S.; Brushett, F. R. An Investigation of the Ionic Conductivity and Species Crossover of Lithiated Nafion 117 in Nonaqueous Electrolytes. *Journal of The Electrochemical Society* **2016**, *163* (1), A5253–A5262. https://doi.org/10.1149/2.03211601jes.

(8) Montoto, E. C.; Nagarjuna, G.; Moore, J. S.; Rodríguez-López, J. Redox Active Polymers for Non-Aqueous Redox Flow Batteries: Validation of the Size-Exclusion Approach. *Journal of The Electrochemical Society* **2017**, *164* (7), A1688–A1694. https://doi.org/10.1149/2.1511707jes.

(9) Gandomi, Y. A.; Aaron, D. S.; Houser, J. R.; Daugherty, M. C.; Clement, J. T.; Pezeshki, A. M.; Ertugrul, T. Y.; Moseley, D. P.; Mench, M. M. Critical Review — Experimental Diagnostics and Material Characterization Techniques Used on Redox Flow Batteries. **2018**, *165* (5), 970–1010. https://doi.org/10.1149/2.0601805jes.

(10) Skyllas-Kozocos, M.; Grossmith, F. Efficient Vanadium Redox Flow Cell. *Journal of the Electrochemical Society* **1987**, *134* (12), 2950–2953. https://doi.org/10.1149/1.2100321.

(11) Taher, M. A.; Majidi, F.; Mohadesi, A. Electrochemical and Electrocatalytic Behaviors of Safranin O/Nafion Film Deposited on the Glassy Carbon Electrode. *Russian Journal of Electrochemistry* **2009**, *45* (10), 1156–1161. https://doi.org/10.1134/S1023193509100073.

(12) Pal, C.; Bandyopadhyay, U. Redox-Active Antiparasitic Drugs. *Antioxidants and Redox Signaling* **2012**, *17* (4), 555–582. https://doi.org/10.1089/ars.2011.4436.

(13) Lv, Y.; Liu, Y.; Feng, T.; Zhang, J.; Lu, S.; Wang, H.; Xiang, Y. Structure Reorganization-Controlled Electron Transfer of Bipyridine Derivatives as Organic Redox Couples. *Journal of Materials Chemistry A* **2019**, *7* (47), 27016–27022. https://doi.org/10.1039/c9ta08910a.

(14) Kosswattaarachchi, A. M.; Cook, T. R. Repurposing the Industrial Dye Methylene Blue as an Active Component for Redox Flow Batteries. *ChemElectroChem* **2018**, *5* (22), 3437–3442. https://doi.org/10.1002/celc.201801097.

(15) Lantz, A. W.; Shavalier, S. A.; Schroeder, W.; Rasmussen, P. G. Evaluation of an Aqueous Biphenol- and Anthraquinone-Based Electrolyte Redox Flow Battery. **2019**. https://doi.org/10.1021/acsaem.9b01381.

(16) Shamsipur, M.; Siroueinejad, A.; Hemmateenejad, B.; Abbaspour, A.; Sharghi, H.; Alizadeh, K.; Arshadi, S. Cyclic Voltammetric, Computational, and Quantitative Structure-Electrochemistry Relationship Studies of the Reduction of Several 9,10-Anthraquinone Derivatives. *Journal of Electroanalytical Chemistry* **2007**, *600* (2), 345–358. https://doi.org/10.1016/j.jelechem.2006.09.006.

(17) Hofmann, J. D.; Pfanschilling, F. L.; Krawczyk, N.; Geigle, P.; Hong, L.; Schmalisch, S.; Wegner, H. A.; Mollenhauer, D.; Janek, J.; Schröder, D. Quest for Organic Active Materials for Redox Flow Batteries: 2,3-Diaza-Anthraquinones and Their Electrochemical Properties. *Chemistry of Materials* **2018**, *30* (3), 762–774. https://doi.org/10.1021/acs.chemmater.7b04220.

(18) Li, Y.; Zuo, P.; Chen, Q.; Sun, P.; Yang, Z.; Xu, T. Screening Viologen Derivatives for Neutral Aqueous Organic Redox Flow Battery. *ChemSusChem* **2020**. https://doi.org/10.1002/cssc.202000381.

(19) Chen, C.; Zhang, S.; Zhu, Y.; Qian, Y.; Niu, Z.; Ye, J.; Zhao, Y.; Zhang, X. Pyridyl Group Design in Viologens for Anolyte Materials in Organic Redox Flow Batteries. *RSC Advances* **2018**, *8* (34), 18762–18770. https://doi.org/10.1039/c8ra02641f.

(20) DeBruler, C.; Hu, B.; Moss, J.; Liu, X.; Luo, J.; Sun, Y.; Liu, T. L. Designer Two-Electron Storage Viologen Anolyte Materials for Neutral Aqueous Organic Redox Flow Batteries. *Chem* **2017**, *3* (6), 961–978. https://doi.org/10.1016/j.chempr.2017.11.001.

(21) Hu, B.; Liu, T. L. Two Electron Utilization of Methyl Viologen Anolyte in Nonaqueous Organic Redox Flow Battery. *Journal of Energy Chemistry* **2018**, *27* (5), 1326–1332. https://doi.org/10.1016/j.jechem.2018.02.014.

(22) Lever, A. B. P. Derivation of Metallophthalocyanine Redox Potentials via Hammett Parameter Analysis. *Inorganica Chimica Acta* **1993**, *203* (2), 171–174.

(23) Zhu, X. Q.; Wang, C. H. Accurate Estimation of the One-Electron Reduction Potentials of Various Substituted Quinones in DMSO and CH_3CN. *The Journal of Organic Chemistry* **2010**, *75* (15), 5037–5047.

(24) Ortiz-Rodríguez, J. C. Santana, J. A.; Méndez-Hernández, D. D. Linear Correlation Models for the Redox Potential of Organic Molecules in Aqueous Solutions. *Journal of Molecular Modeling* **2020**, *26* (4), 1–8.

(25) Méndez-Hernández, D. D.; Gillmore, J. G.; Montano, L. A.; Gust, D.; Moore, T. A.; Moore, A. L.; Mujica, V. Building and Testing Correlations for the Estimation of One-electron Reduction Potentials of a Diverse Set of Organic Molecules. *Journal of Physical Organic Chemistry* **2015**, *28* (5), 320–328.

(26) Marenich, A. V.; Ho, J.; Coote, M. L.; Cramer, C. J.; Truhlar, D. G. Computational Electrochemistry: Prediction of Liquid-Phase Reduction Potentials. *Physical Chemistry Chemical Physics* **2014**, *16* (29), 15068–15106. https://doi.org/10.1039/c4cp01572j.

(27) Pelzer, K. M.; Cheng, L.; Curtiss, L. A. Effects of Functional Groups in Redox-Active Organic Molecules: A High-Throughput Screening Approach. *Journal of Physical Chemistry C* **2017**, *121* (1), 237–245. https://doi.org/10.1021/acs.jpcc.6b11473.

(28) Er, S.; Suh, C.; Marshak, M. P.; Aspuru-Guzik, A. Computational Design of Molecules for an All-Quinone Redox Flow Battery. *Chemical Science* **2015**, *6* (2), 885–893. https://doi.org/10.1039/c4sc03030c.

(29) Moon, Y.; Han, Y. K. Computational Screening of Organic Molecules as Redox Active Species in Redox Flow Batteries. *Current Applied Physics* **2016**, *16* (9), 939–943. https://doi.org/10.1016/j.cap.2016.05.012.

(30) Fu, Y.; Liu, L.; Yu, H. Z.; Wang, Y. M.; Guo, Q. X. Quantum-Chemical Predictions of Absolute Standard Redox Potentials of Diverse Organic Molecules and Free Radicals in Acetonitrile. *Journal of the American Chemical Society* **2005**, *127* (19), 7227–7234. https://doi.org/10.1021/ja0421856.

(31) Schmidt Am Busch, M.; Knapp, E. W. One-Electron Reduction Potential for Oxygen- and Sulfur-Centered Organic Radicals in Protic and Aprotic Solvents. *Journal of the American Chemical Society* **2005**, *127* (45), 15730–15737. https://doi.org/10.1021/ja0526923.

(32) Blinco, J. P.; Hodgson, J. L.; Morrow, B. J.; Walker, J. R.; Will, G. D.; Coote, M. L.; Bottle, S. E. Experimental and Theoretical Studies of the Redox Potentials of Cyclic Nitroxides. *Journal of Organic Chemistry* **2008**, *73* (17), 6763–6771. https://doi.org/10.1021/jo801099w.

(33) Namazian, M.; Coote, M. L. Accurate Calculation of Absolute One-Electron Redox Potentials of Some Para-Quinone Derivatives in Acetonitrile. *Journal of Physical Chemistry A* **2007**, *111* (30), 7227–7232. https://doi.org/10.1021/jp0725883.

(34) Huynh, M. T.; Anson, C. W.; Cavell, A. C.; Stahl, S. S.; Hammes-Schiffer, S. Quinone 1 e- and 2 e-/2 H^+ Reduction Potentials: Identification and Analysis of Deviations from Systematic Scaling Relationships. *Journal of the American Chemical Society* **2016**, *138* (49), 15903–15910. https://doi.org/10.1021/jacs.6b05797.

(35) Sterling, C. M.; Bjornsson, R. Multistep Explicit Solvation Protocol for Calculation of Redox Potentials. *Journal of Chemical Theory and Computation* **2019**, *15* (1), 52–67. https://doi.org/10.1021/acs.jctc.8b00982.

(36) Huang, J.; Yang, Z.; Murugesan, V.; Walter, E.; Hollas, A.; Pan, B.; Assary, R. S.; Shkrob, I. A.; Wei, X.; Zhang, Z. Spatially Constrained Organic Diquat Anolyte for Stable Aqueous Flow Batteries. *ACS Energy Letters* **2018**, *3* (10), 2533–2538. https://doi.org/10.1021/acsenergylett.8b01550.

(37) Isegawa, M.; Neese, F.; Pantazis, D. A. Ionization Energies and Aqueous Redox Potentials of Organic Molecules: Comparison of DFT, Correlated Ab Initio Theory and Pair Natural Orbital Approaches. *Journal of Chemical Theory and Computation* **2016**, *12* (5), 2272–2284. https://doi.org/10.1021/acs.jctc.6b00252.

(38) Shao, Y.; Gan, Z.; Epifanovsky, E.; Gilbert, A. T. B.; Wormit, M.; Kussmann, J.; Lange, A. W.; Behn, A.; Deng, J.; Feng, X.; *et al.* Advances in Molecular Quantum Chemistry Contained in the Q-Chem 4 Program Package. *Molecular Physics* **2015**, *113* (2), 184–215. https://doi.org/10.1080/00268976.2014.952696.

(39) Marković, Z.; Tošović, J.; Milenković, D.; Marković, S. Revisiting the Solvation Enthalpies and Free Energies of the Proton and Electron in Various Solvents. *Computational and Theoretical Chemistry* **2016**, *1077*, 11–17. https://doi.org/10.1016/j.comptc.2015.09.007.

(40) Pavlishchuk, V. V.; Addison, A. W. Conversion Constants for Redox Potentials Measured versus Different Reference Electrodes in Acetonitrile Solutions at 25°C. *Inorganica Chimica Acta* **2000**, *298* (1), 97–102. https://doi.org/10.1016/S0020-1693(99)00407-7.

(41) Singh, A.; Chowdhury, D. R.; Paul, A. A Kinetic Study of Ferrocenium Cation Decomposition Utilizing an Integrated Electrochemical Methodology Composed of Cyclic Voltammetry and Amperometry. *Analyst* **2014**, *139* (22), 5747–5754. https://doi.org/10.1039/c4an01325e.

(42) Konezny, S. J.; Doherty, M. D.; Luca, O. R.; Crabtree, R. H.; Soloveichik, G. L.; Batista, V. S. Reduction of Systematic Uncertainty in DFT Redox Potentials of Transition-Metal Complexes. *Journal of Physical Chemistry C* **2012**, *116* (10), 6349–6356. https://doi.org/10.1021/jp300485t.

(43) Wang, H.; Emanuelsson, R.; Banerjee, A.; Ahuja, R.; Strømme, M.; Sjö; Din, M. Effect of Cycling Ion and Solvent on the Redox Chemistry of Substituted Quinones and Solvent-Induced Breakdown of the Correlation Between Redox Potential and Electron Withdrawing Power of Substituents. *The Journal of Physical Chemistry C* **2020**. https://doi.org/10.1021/acs.jpcc.0c03632.

(44) Kottam, P. K. R.; Kalkan, D.; Wohlfahrt-Mehrens, M.; Marinaro, M. Influence of Li-Salt Concentration on Redox Potential of Lithium Metal and Electrochemistry of Ferrocene in DMSO-Based Electrolytes. *Journal of The Electrochemical Society* **2019**, *166* (8), A1574–A1579. https://doi.org/10.1149/2.0881908jes.

(45) Silvester, D. S.; Wain, A. J.; Aldous, L.; Hardacre, C.; Compton, R. G. Electrochemical Reduction of Nitrobenzene and 4-Nitrophenol in the Room Temperature Ionic Liquid [C4dmim][N(Tf)2]. *Journal of Electroanalytical Chemistry* **2006**, *596* (2), 131–140. https://doi.org/10.1016/j.jelechem.2006.07.028.

(46) Tocher, J. H.; Edwards, D. I. Electrochemical Characteristics of Nitroheterocyclic Compounds of Biological Interest I. The Influence of Solvent. *Free Radical Research* **1988**, *4* (5), 269–276. https://doi.org/10.3109/10715769009148572.

(47) Speer, M. E.; Kolek, M.; Jassoy, J. J.; Heine, J.; Winter, M.; Bieker, P. M.; Esser, B. Thianthrene-Functionalized Polynorbornenes as High-Voltage Materials for Organic Cathode-Based Dual-Ion Batteries. *Chemical Communications* **2015**, *51* (83), 15261–15264. https://doi.org/10.1039/c5cc04932f.

(48) Papajak, E.; Truhlar, D. G. Efficient Diffuse Basis Sets for Density Functional Theory. *Journal of Chemical Theory and Computation* **2010**, *6* (3), 597–601. https://doi.org/10.1021/ct900566x.

(49) Lynch, B. J.; Zhao, Y.; Truhlar, D. G. Effectiveness of Diffuse Basis Functions for Calculating Relative Energies by Density Functional Theory. *Journal of Physical Chemistry A* **2003**, *107* (9), 1384–1388. https://doi.org/10.1021/jp021590l.

(50) Gronert, S. The Need for Additional Diffuse Functions in Calculations on Small Anions: The G2(Dd) Approach. *Chemical Physics Letters* **1996**, *252* (5–6), 415–418. https://doi.org/10.1016/0009-2614(96)00162-5.

(51) Jakubikova, E.; Rappé, A. K.; Bernstein, E. R. Exploration of Basis Set Issues for Calculation of Intermolecular Interactions. *Journal of Physical Chemistry A* **2006**, *110* (31), 9529–9541. https://doi.org/10.1021/jp0680239.

(52) Aissing, G.; Monkhorst, H. J. Linear Dependence in Basis-set Calculations for Extended Systems. *International Journal of Quantum Chemistry* **1992**, *43* (6), 733–745. https://doi.org/10.1002/qua.560430602.

(53) Moncrieff, D.; Wilson, S. Computational Linear Dependence in Molecular Electronic Structure Calculations Using Universal Basis Sets. *International Journal of Quantum Chemistry* **2005**, *101* (4), 363–371. https://doi.org/10.1002/qua.20275.

(54) Madrid-Úsuga, D.; Melo-Luna, C. A.; Insuasty, A.; Ortiz, A.; Reina, J. H. Optical and Electronic Properties of Molecular Systems Derived from Rhodanine. *Journal of Physical Chemistry A* **2018**, *122* (43), 8469–8476. https://doi.org/10.1021/acs.jpca.8b08265.

(55) Kelly, C. P.; Cramer, C. J.; Truhlar, D. G. Aqueous Solvation Free Energies of Ions and Ion-Water Clusters Based on an Accurate Value for the Absolute Aqueous Solvation Free Energy of the Proton. *Journal of Physical Chemistry B* **2006**, *110* (32), 16066–16081. https://doi.org/10.1021/jp063552y.

(56) Tissandier, M. D.; Cowen, K. A.; Feng, W. Y.; Gundlach, E.; Cohen, M. H.; Earhart, A. D.; Coe, J. V.; Tuttle, T. R. The Proton's Absolute Aqueous Enthalpy and Gibbs Free Energy of Solvation from Cluster-Ion Solvation Data. *Journal of Physical Chemistry A* **1998**, *102* (40), 7787–7794. https://doi.org/10.1021/jp982638r.

ToC Graphic

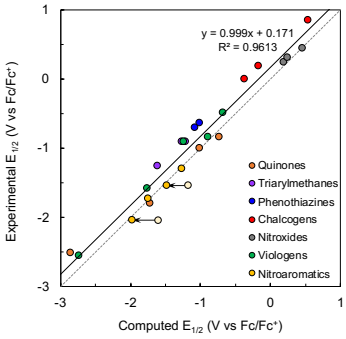
y = 0.999x + 0.171
R² = 0.9613
Quinones
Triarylmethanes
Phenothiazines
Chalcogens
Nitroxides
Viologens
Nitroaromatics
Experimental E1/2 (V vs Fc/Fc+)
Computed E1/2 (V vs Fc/Fc+)
1
0
-1
-2
-3
-3
-2
-1
0
1